5. C. F. Boerkoel *et al.*, *Nat. Genet.* **30**, 215 (2002).
6. The turnover number (k_{cat}) values (mean ± SD; $N = 4$) for HARP ATPase activity with fork DNA and dsDNA are approximately 1200 ± 270 min^{-1} and 81 ± 29 min^{-1}, respectively. ATPase activity was not detectable in the absence of DNA or in the presence of ssDNA.
7. R. Muthuswami, P. A. Truman, L. D. Mesner, J. W. Hockensmith, *J. Biol. Chem.* **275**, 7648 (2000).
8. J. W. Hockensmith, A. F. Wahl, S. Kowalski, R. A. Bambara, *Biochemistry* **25**, 7812 (1986).
9. L. Wu, I. D. Hickson, *Annu. Rev. Genet.* **40**, 279 (2006).
10. A. Georgaki, B. Strack, V. Podust, U. Hübscher, *FEBS Lett.* **308**, 240 (1992).
11. K. Treuner, U. Ramsperger, R. Knippers, *J. Mol. Biol.* **259**, 104 (1996).
12. Y. Lao, C. G. Lee, M. S. Wold, *Biochemistry* **38**, 3974 (1999).
13. D. T. Auble, D. Wang, K. W. Post, S. Hahn, *Mol. Cell. Biol.* **17**, 4842 (1997).
14. J. J. Chicca 2nd, D. T. Auble, B. F. Pugh, *Mol. Cell. Biol.* **18**, 1701 (1998).
15. A. Saha, J. Wittmeyer, B. R. Cairns, *Genes Dev.* **16**, 2120 (2002).
16. M. Jaskelioff, S. Van Komen, J. E. Krebs, P. Sung, C. L. Peterson, *J. Biol. Chem.* **278**, 9212 (2003).
17. I. Amitani, R. J. Baskin, S. C. Kowalczykowski, *Mol. Cell* **23**, 143 (2006).
18. P. McGlynn, R. G. Lloyd, *Cell* **101**, 35 (2000).
19. C. Ralf, I. D. Hickson, L. Wu, *J. Biol. Chem.* **281**, 22839 (2006).
20. A. Blastyák *et al.*, *Mol. Cell* **28**, 167 (2007).
21. L. I. Elizondo *et al.*, *Am. J. Med. Genet.* **140A**, 340 (2006).
22. We thank B. Rattner, J.-Y. A. Hsu, T. Juven-Gershon, D. Urwin, and J. Theisen for critical reading of the manuscript; M. Coleman for the gift of HARP cDNAs in the early stages of this study; M. Wold for the human RPA expression vector; B. Cairns for the triple-helix plasmid; R. Kingston for the BRG1 expression vector; and M. Gellert for a helpful discussion on this work prior to publication. Supported by NIH grant GM058272 (J.T.K.) and by NIH National Research Service Award fellowship F32 GM76936 (T.Y.).

Supporting Online Material

www.sciencemag.org/cgi/content/full/322/5902/748/DC1
Materials and Methods
Figs. S1 to S13
References

2 June 2008; accepted 25 September 2008
10.1126/science.1161233

Polycomb Proteins Targeted by a Short Repeat RNA to the Mouse X Chromosome

Jing Zhao,[1,2,3] Bryan K. Sun,[1,2,3] Jennifer A. Erwin,[1,2,3] Ji-Joon Song,[2,3] Jeannie T. Lee[1,2,3]*

To equalize X-chromosome dosages between the sexes, the female mammal inactivates one of her two X chromosomes. X-chromosome inactivation (XCI) is initiated by expression of *Xist*, a 17-kb noncoding RNA (ncRNA) that accumulates on the X in cis. Because interacting factors have not been isolated, the mechanism by which *Xist* induces silencing remains unknown. We discovered a 1.6-kilobase ncRNA (RepA) within *Xist* and identified the Polycomb complex, PRC2, as its direct target. PRC2 is initially recruited to the X by RepA RNA, with Ezh2 serving as the RNA binding subunit. The antisense *Tsix* RNA inhibits this interaction. RepA depletion abolishes full-length *Xist* induction and trimethylation on lysine 27 of histone H3 of the X. Likewise, PRC2 deficiency compromises *Xist* up-regulation. Therefore, RepA, together with PRC2, is required for the initiation and spread of XCI. We conclude that a ncRNA cofactor recruits Polycomb complexes to their target locus.

The mouse X-chromosome inactivation (XCI) center harbors several noncoding genes, including *Xist* (*1*, *2*) and its antisense repressor, *Tsix* (*3*). On the future Xa (active X), *Tsix* blocks *Xist* up-regulation and prevents the recruitment of silencing factors in cis. On the future Xi (inactive X), *Tsix* is down-regulated, which enables *Xist* transactivation and the spread of Xist RNA along the chromosome (*4*). The accumulation of *Xist* transcripts correlates with a cascade of chromatin changes (*5*), but how *Xist* directs these changes is unknown. In principle, the act of transcribing *Xist* could induce structural changes that could alter chromosomewide function (*1*). Alternatively, *Xist* could work as a transcript (*1*, *2*) by recruiting chromatin modifiers or by targeting the X to a specialized compartment (*6*). Although universally attractive, RNA-based models have remained hypothetical, as Xist-interacting proteins have yet to be identified.

[1]Howard Hughes Medical Institute, Boston, MA 02115, USA. [2]Department of Molecular Biology, Massachusetts General Hospital, Boston, MA 02493, USA. [3]Department of Genetics, Harvard Medical School, Boston, MA 02115, USA.

*To whom correspondence should be addressed. E-mail: lee@molbio.mgh.harvard.edu

To circumvent conventional difficulties with purifying Xist-interacting proteins, we carried out RNA immunoprecipitations (RIPs) and asked if Xist RNA can be found in a specific protein complex. We isolated nuclear RNAs and their binding proteins in the native state to avoid fixation artifacts and tested two cell types: mouse embryonic stem (ES) cells, which exist in the pre-XCI state but recapitulate XCI when induced to differentiate, and mouse embryonic fibroblasts (MEFs), which faithfully maintain Xi. Because trimethylation of histone 3 at Lys^{27} (H3-K27me3) closely follows *Xist* up- and down-regulation (*6*–*9*), we asked if Xist RNA binds the H3-K27 methylase, PRC2—the Polycomb complex that includes Eed, Suz12, RbAp48, and the catalytic subunit, Ezh2 (*10*). Indeed, Ezh2 and Suz12 antibodies coimmunoprecipitated Xist RNA (Fig. 1, A to D). By contrast, Xist sequences were not consistently detected in cells treated with antibodies against H3-K27me3 or antibodies against acetylated H4, or in no-antibody controls. Pretreatment with ribonucleases (RNases) that digest single-stranded RNA (RNase I) and double-stranded RNA (RNase V1) abolished RIP signals, whereas pretreatment with RNase H (which digests RNA in RNA:DNA hybrids), DNase I, or no nucleases had no effect (Fig. 1E). By inference, the RIP products must be single- or double-stranded RNA.

In female cells, RNA could be detected in the complex even in the pre-XCI state (day 0) when there are <10 transcripts per cell (*11*). On day 0, PRC2 bound only Repeat A (R1), a motif required for silencing (*12*, *13*). Quantitative strand-specific RIP showed that both sense and antisense strands were highly enriched in the PRC2 complex (Fig. 1F). Not until cell differentiation and *Xist* up-regulation could PRC2 coimmunoprecipitate more 3′ regions of *Xist*, which suggested that other regions of Xist eventually come in contact with PRC2, though Repeat A remained the epicenter of binding (Fig. 1G). To determine when PRC2 is loaded onto chromatin, we performed DNA chromatin immunoprecipitation (ChIP) assays (Fig. 1H). While bound to RNA in day 0 wild-type cells, PRC2 was not enriched on DNA until differentiation (day 3, day 6) when Eed and/or Ezh2 levels increased ~10-fold. Accordingly, H3-K27me3 levels rose >10-fold. Together, RIP and ChIP showed that, although PRC2 bound Repeat A in pre-XCI cells, H3-K27me3 of chromatin was not evident until differentiation (Fig. 1, B and H). For males, PRC2 coimmunoprecipitated Xist sequences only in ES cells, not in MEFs (Fig. 1C), consistent with the absence of XCI. In $Tsix^{\Delta CpG/+}$ female cells, where XCI choice is predetermined and accelerated (*3*), PRC2 spreading occurred earlier, consistent with preemptive H3-K27me3 (Fig. 1, D and H) (*11*). Thus, PRC2 recruitment by RNA and its activity on chromatin are biochemically separable.

Examination of $Tsix^{\Delta CpG/+}$ cells enabled us to determine when *Xist* transactivation occurred relative to PRC2 recruitment. In this mutant, XCI always occurs on the mutated X, and H3-K27 methylation preempts *Xist* up-regulation, which indicated that H3-K27me3 and *Xist* transactivation are genetically separable (*11*). Indeed, DNA ChIP showed high Eed and Ezh2 enrichment on Repeat A on day 0 with accompanying H3-K27me3 (Fig. 1H). *Xist* expression remained low until differentiation (*11*). Therefore, in wild-type cells, PRC2 is recruited by RNA to *Xist*'s 5′ end on day 0, but PRC2

transfers to chromatin and catalyzes H3-K27me3 only after differentiation is triggered. These events occur before *Xist* transactivation.

Note that PRC2 preferentially associates with Repeat A across all time points (Fig. 1G), although PRC2 should theoretically coimmunoprecipitate all regions of an intact Xist molecule during native RIP, regardless of which RNA domain binds PRC2. To undertake higher-resolution analysis, we performed Xist-strand quantitative polymerase chain reaction (PCR) between *Xist* promoters P1 and P2 in ES cells and observed RNA levels at R7 and R8 three to four times as great as at R6 and R9 (Fig. 2, A and B). During differentiation, *Xist* up-regulated >100-fold in females but became barely detectable in males (Fig. 2C).

Quantitative differences at R6 to R9 hinted at a novel promoter activity. Indeed, RNA fluorescence in situ hybridization (FISH) detected a pinpoint signal on day 0 (Fig. 2D). Northern analysis revealed a ~1.6-kb transcript, with no obvious antisense counterparts other than known processed *Tsix* transcripts (Fig. 2E) (*14*). Rapid amplification of cDNA 3′ ends (3′ RACE) de-

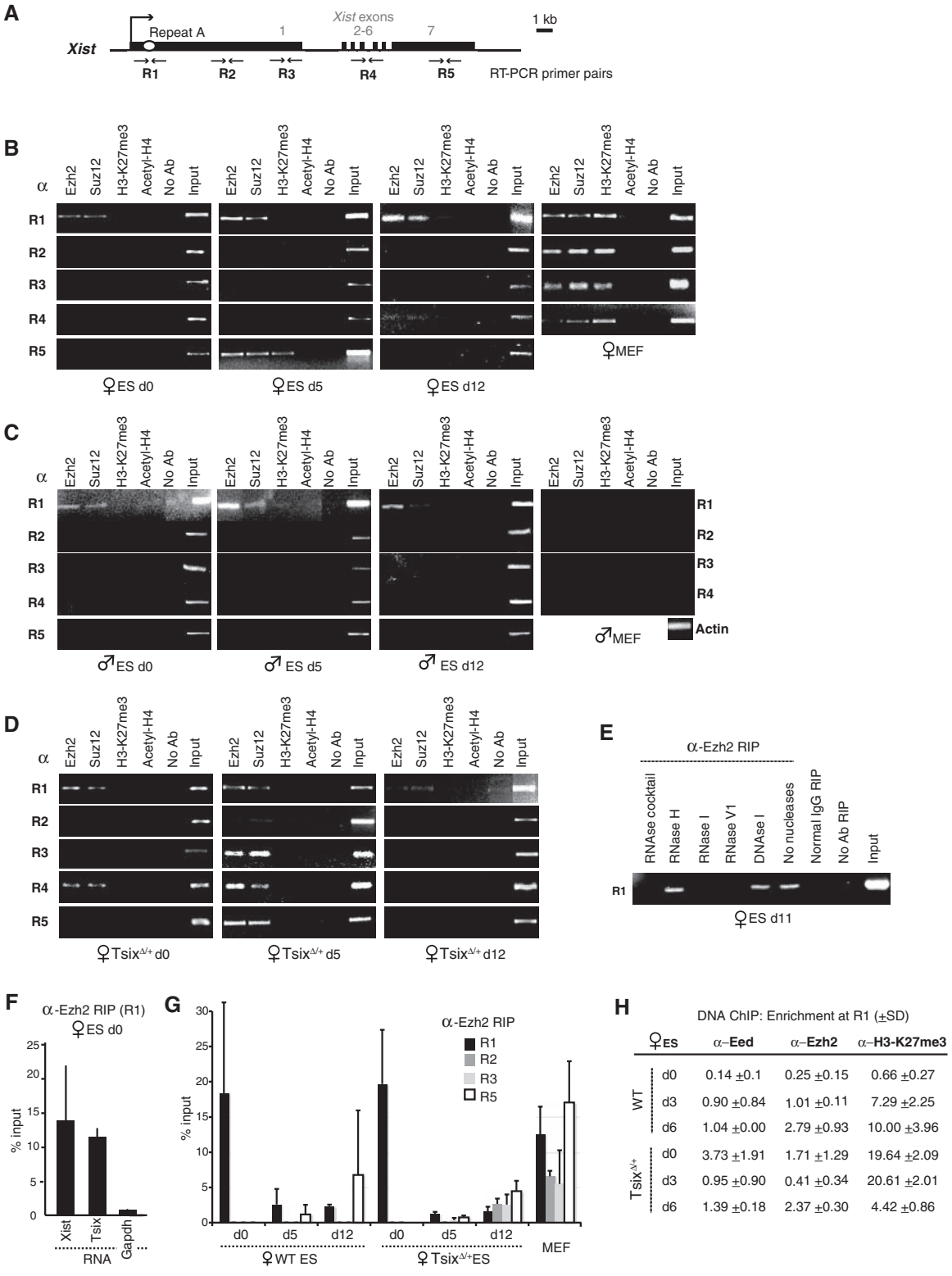

Fig. 1. The PRC2 complex contains Xist. (**A**) Map of *Xist*. (**B** to **D**) RIP in indicated cells. α, antibodies. (**E**) Effects of RNase pretreatment on RIP signals. (**F**) Strand-specific RIP at R1 by real-time PCR, normalized to input RNA. Error bar, 1 SD. (**G**) Quantitative RIP by real-time PCR at positions R1 to R5. (**H**) DNA ChIP using indicated antibodies, shown as a fraction of input and standardized to normal IgG ChIP. Day 0, d0, and so on.

fined its terminus at base pair (bp) 1948 downstream of P1 (Fig. 2F), which implied a transcription start site at ~bp 300. Luciferase reporter assays confirmed promoter activity within bp 79 to 320, appearing equally active in pre- and post-XCI cells, whereas P1 activity increased upon XCI (Fig. 2G). Competitive reverse transcription PCR (RT-PCR) previously revealed ~10 absolute copies of sense RNA in this region in day 0 female ES cells (*11*). The current stoichiometric data implied that three or four copies derive from full-length *Xist* and six or seven from Repeat A (Fig. 2B). Upon differentiation, Xist levels increased ~100-fold (Fig. 2C), whereas Repeat A levels increased 1.8-fold (Fig. 2E). Thus, Repeat A produces a small internal transcript, present in both male and female cells before XCI, but restricted to females after XCI. We designate the transcript "RepA" for Repeat A.

To test whether PRC2 is actually recruited by RepA, we generated doxycycline-inducible *RepA* transgenic female ES cells (Fig. 2H) and asked whether RepA could target PRC2 to ectopic autosomal sites independently of *Xist*. Indeed, for two clones (B5 and C5) of low transgene copy number, doxycycline induction resulted in about a threefold increase in RepA and commensurate increases in PRC2 binding (Fig. 2I). Thus, RepA is sufficient to recruit PRC2 in vivo without Xist, and recruitment depends on RepA transcription and/or RNA.

Does RepA RNA directly bind PRC2? To investigate, we tested whether RepA RNA oligomers could shift PRC2 in vitro in an electrophoretic mobility shift assay (EMSA). RepA comprises 7.5 tandem repeats of a 28-nucleotide (nt) se-

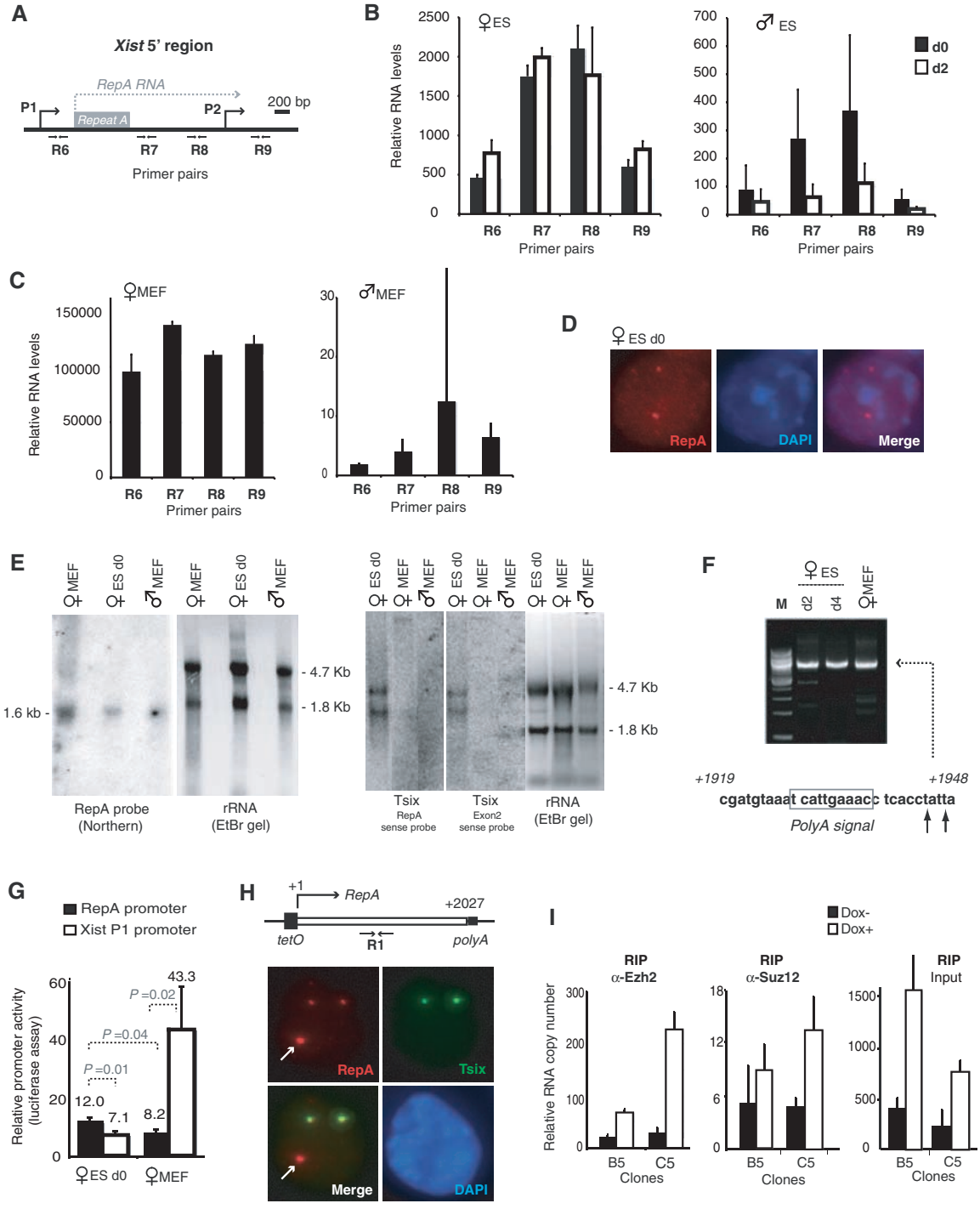

Fig. 2. A small RNA within *Xist*. (**A**) Map of *RepA* and the 5′ end of *Xist*. (**B** and **C**). Strand-specific real-time PCR quantifies RNA copies at R6 to R9 in ES cells (B) or MEFs (C), normalized to standard curve. (**D**) RNA FISH using RepA probe. (**E**) Northern analysis of RepA and Tsix (5′ and 3′ positions). (**F**) 3′ RACE of RepA. (**G**) Transient transfection of luciferase reporter constructs comparing RepA (bp 79 to 320) versus *Xist* P1 promoters, each normalized to vector control. *P*, Student's *t* tests in indicated pairwise comparisons. (**H**) DNA FISH of *RepA* transgenic female ES cells. *Xist* P1 promoter is not in transgenes. Arrows, transgene. *Tsix* detected by pSx7. (**I**) Quantitative RIP in representative clones B5 and C5 ± doxycycline induction. No-antibody controls yielded no detectable RNA.

quence that folds into two conserved stem-loop structures (*13*) (Fig. 3A). A specific RNA-protein complex was observed when ES cell nuclear extract was incubated with wild-type sense probe (Fig. 3, B and C). It is noteworthy that a specific complex was also seen with antisense RNA, which harbors complementary stem-loop structures. In both cases, RNA-protein interactions were disrupted by excess cold wild-type, but not mutant or random, competitors. No shift was observed with a mutant probe lacking the conserved stem-loop structures or with random RNA oligomers (DsI and DsII). Therefore, a specific factor in ES cell nuclei binds RepA and Tsix.

To identify the factor, we asked if antibodies against Ezh2 could supershift the complex and found that preincubation in nuclear extract (day 4 female ES cells or MEFs) produced a supershift, whereas normal immunoglobulin IgG did not (Fig. 3D). Therefore, PRC2 directly binds RepA and Tsix, in agreement with RIP results (Fig. 1F). To confirm, we generated recombinant human PRC2 (hPRC2) containing EED, EZH2, SUZ12, and RBAP48 (*15*) and observed that hPRC2 shifted both sense and antisense RNAs but not mutated or random RNA [(Fig. 3, E and F) additional bands may indicate subcomplexes]. The hEED-hEZH2 subcomplex and the complete hPRC2 complex bound wild-type RNAs equally well. Ezh2 alone could also bind RNA, but hEED alone could not. Thus, Ezh2 must be the RNA-binding subunit of PRC2 (fig. S1). Given that Tsix also binds PRC2 and is a known *Xist* antagonist, Tsix could block XCI by titrating away PRC2. Indeed, RepA and Tsix oligomers competed with each other for PRC2 in vitro (Fig. 3C) and, in

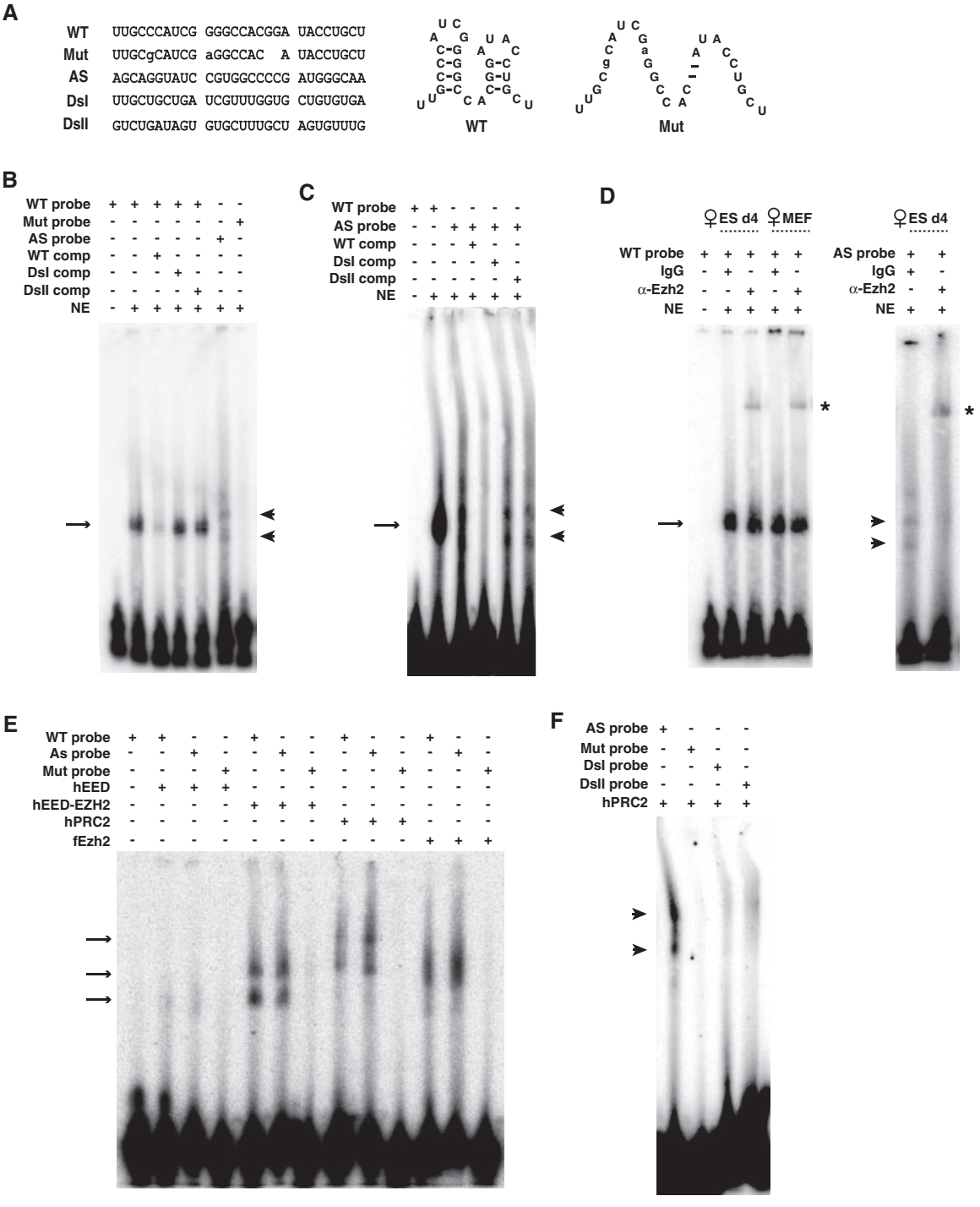

Fig. 3. RepA RNA directly binds PRC2 in vitro. (**A**) One Repeat A unit. WT, wild-type sense; mut, mutated; and AS, antisense. DsI and DsII, randomized *Xist* sequences. (**B**) EMSA using female ES cell nuclear extract (NE). Comp, competitors at 500× molar excess. Arrow, sense shift; arrowhead, antisense shift. (**C**) Antisense binding competed by sense RNAs but not nonspecific RNAs. (**D**) EMSA supershifts (*) with antibodies against Ezh2. (**E**) EMSA using recombinant hPRC2 (sub)complexes. fEzh2, *Drosophila* Ezh2. (**F**) hPRC2 bound by antisense but not by randomized probes.

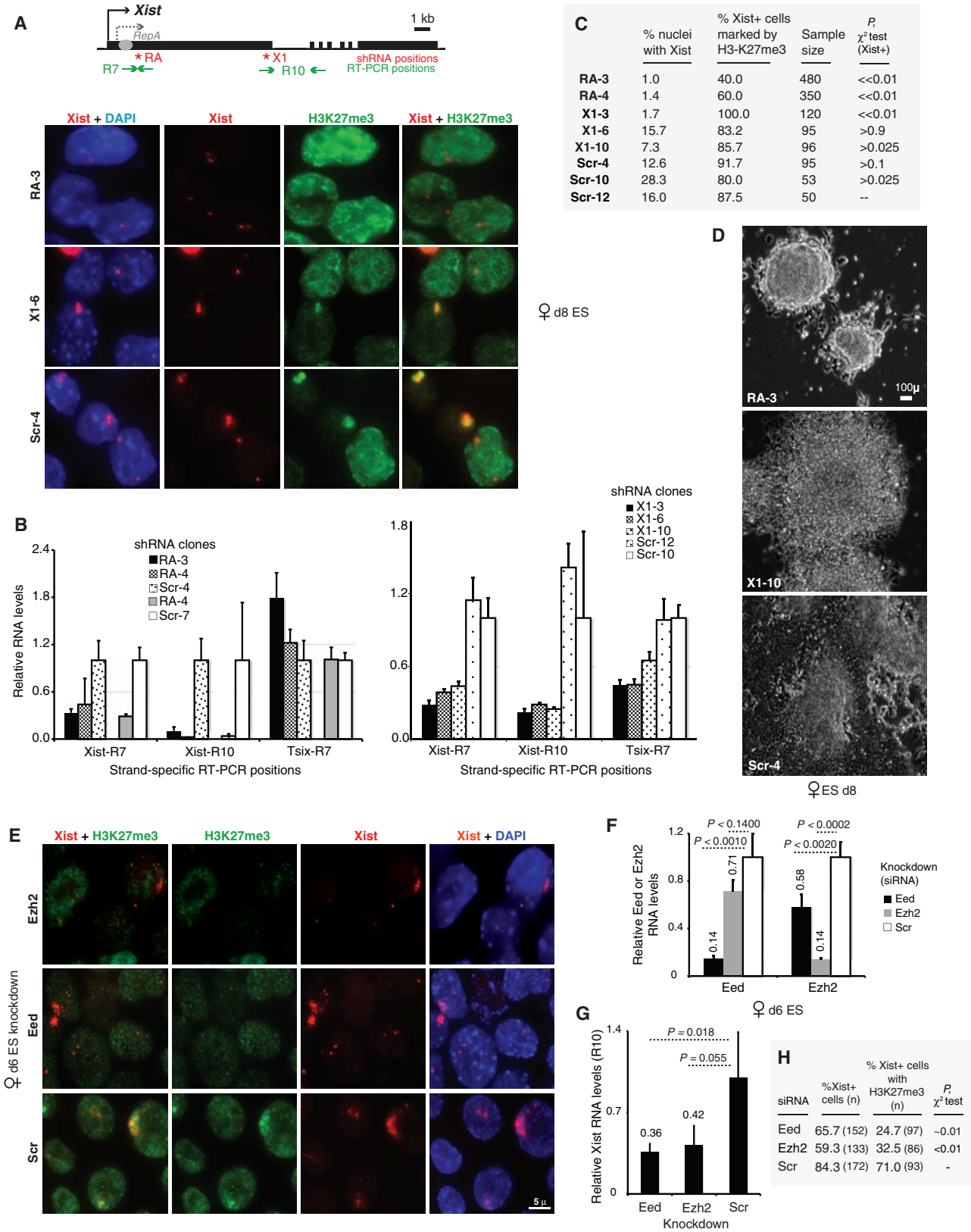

C

	% nuclei with Xist	% Xist+ cells marked by H3-K27me3	Sample size	P, χ^2 test (Xist+)
RA-3	1.0	40.0	480	<<0.01
RA-4	1.4	60.0	350	<<0.01
X1-3	1.7	100.0	120	<<0.01
X1-6	15.7	83.2	95	>0.9
X1-10	7.3	85.7	96	>0.025
Scr-4	12.6	91.7	95	>0.1
Scr-10	28.3	80.0	53	>0.025
Scr-12	16.0	87.5	50	--

H

siRNA	%Xist+ cells (n)	% Xist+ cells with H3K27me3 (n)	P, χ^2 test
Eed	65.7 (152)	24.7 (97)	~0.01
Ezh2	59.3 (133)	32.5 (86)	<0.01
Scr	84.3 (172)	71.0 (93)	-

Fig. 4. RepA/PRC2 knockdowns compromise XCI initiation. (**A**) Xist RNA–H3-K27me3 immunoFISH in knockdown clones. ShRNA: RA, RepA. X1, *Xist* exon 1, Scr, scrambled control. (**B**) Xist and Tsix levels at indicated positions in knockdown clones. (**C**) ImmunoFISH: Frequency of *Xist* up-regulation (*Xist*$^+$) and H3-K27me3 foci. *P*, pairwise comparison against Scr-12 control for *Xist*$^+$ frequencies. (**D**) Embryoid body growth in shRNA clones. (**E**) Xist–H3-K27me3 immunoFISH after Eed, Ezh2, or control knockdown. (**F**) Eed and Ezh2 mRNA levels after knockdown in *Tsix*$^{\Delta/+}$ ES cells. *P*, *t* test. (**G**) Quantitative RT-PCR of Xist RNA after indicated knockdowns. *P*, *t* test. (**H**) ImmunoFISH: Frequency of *Xist* up-regulation and H3-K27 trimethylation after indicated knockdowns. *P* compares Xist foci numbers in controls ("expected") versus Eed/Ezh2 knockdowns.

the absence of Tsix in vivo ($Tsix^{\Delta CpG/+}$), H3-K27me3 occurred prematurely on day 0 (Fig. 1H). We propose that RepA directly interacts with Ezh2 and that Tsix competitively inhibits this interaction. As full-length Xist also contains the Repeat A motif, it is likely that Xist RNA also directly interacts with PRC2. Consistent with this idea, PRC2 coimmunoprecipitates both 5′ and 3′ domains of Xist RNA in RIP analysis (Fig. 1, B to D).

Previously, PRC2 seemed an unlikely direct target of Xist, as one report suggested that PRC2 is recruited without Repeat A (*7*). However, another report showed that PRC2 recruitment drops 80 to 90% in Repeat A mutants (*9*). To test if RepA functions in XCI, we created female ES clones carrying short hairpin RNA (shRNA) transgenes directed against *RepA* (RA clones) (Fig. 4A). Because RepA and Xist overlap, shRNA against RepA could potentially affect Xist. To distinguish RepA from Xist, we created shRNA against the end of *Xist* exon 1 (X1), which does not overlap RepA. Quantitative RT-PCR confirmed knockdown efficacy and specificity [(Fig. 4B) Xist contains the R7 sequence, so it may be affected by X1 knockdown; residual R7 levels may represent RepA].

Xist induction was severely compromised when RepA was depleted in clones RA-3 and RA-4, as few Xist foci were seen on day 8 when compared with X1 and scrambled (Scr) controls (Fig. 4, A to C). Thus, RepA RNA is required for *Xist* up-regulation. In 100% of RA-3 and RA-4 cells lacking Xist foci, H3-K27me3 was absent on the X (Fig. 4C). In a very small minority of RA-3 and RA-4 cells that up-regulated *Xist*, H3-K27me3 was also compromised, which indicated PRC2 recruitment defects—high Xist levels notwithstanding. Consistent with the failure of XCI, RepA-shRNA clones showed extremely poor embryoid body differentiation in contrast to controls (Fig. 4D). X1 clones showed an intermediate phenotype, consistent with intermediate expression of *Xist*. Although the X1 region is dispensable for silencing and localization (*13*), its knockdown could affect overall Xist stability and might explain the intermediate phenotype. We conclude that RepA RNA functions not only in Xist transactivation but also in H3-K27 methylation and XCI.

We next examined whether knocking down PRC2 subunits might have similar effects. Indeed, Eed and Ezh2 knockdown in day 6 female embryoid body led to significant reductions in Xist and H3-K27me3 foci (Fig. 4, E to H). Therefore, PRC2 also plays a role in *Xist* up-regulation and XCI. Consistent with previous studies (*16*, *17*), among $Xist^{+}$ cells, PRC2 deficiency did not abrogate gene silencing (fig. S2), possibly because of functional redundancy of PRC2 and PRC1 (*17*). By our data (Figs. 1H and 4), the primary effect of the RepA-PRC2 knockdowns may be abrogation of preemptive H3-K27me3 on *Xist*, an event hypothesized to be

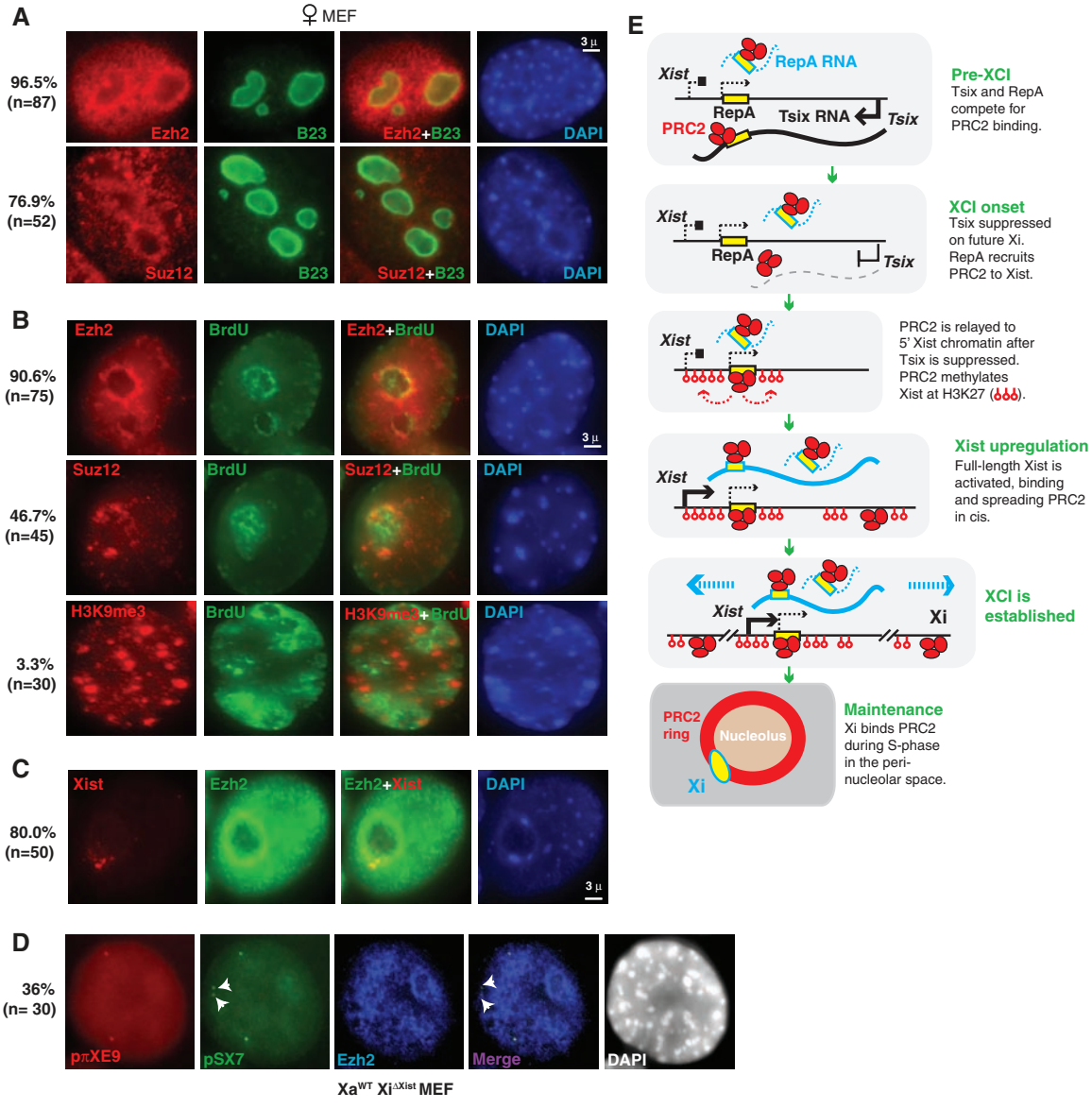

Fig. 5. PRC2 and Xi associate in the perinucleolar compartment after XCI. (**A**) Immunostain: Ezh2 and Suz12 concentrate around the nucleolus (B23+). (**B**) Ezh2 and Suz12, but not H3-K9me3, showed perinucleolar enrichment. (**C**) Xist RNA-Ezh2 immunoFISH. (**D**) *Xist* DNA-Ezh2 immunoFISH in $Xa^{WT}Xi^{\Delta Xist}$ MEFs (*6*). (**E**) Summary and model.

necessary for *Xist* induction (*11*). Therefore, RepA-PRC2 complex may act during XCI, firstly by inducing H3-K27me3 at *Xist* for its transactivation and secondly by enabling spread of H3-K27me3 along the Xi.

Given the importance of PRC2, it is odd that Xi is decorated by PRC2 only during initiation of XCI, though it stably retains H3-K27me3 thereafter (*7*, *8*). Given the hypothesis that Xi's epigenetic state is maintained by visiting a perinucleolar compartment during S phase (*6*), we wondered if PRC2 association during the maintenance phase may be likewise compartmentalized and transient. Indeed, we observed high levels of Ezh2 and Suz12 in this late-replicating perinucleolar compartment (Fig. 5, A and B), to which ~80% of Xi is associated in MEFs (Fig. 5C). When Xi has *Xist* deleted after XCI ($Xa^{WT}Xi^{\Delta Xist}$), the chromosome fails to relocalize to this compartment (*6*). In such cells, we observed that perinucleolar localization and H3-K27me3 were abolished (Fig. 5D) (*6*), which supports the idea that Xi in post-XCI cells associates with PRC2 and maintains H3-K27me3 by visiting the perinucleolar compartment during DNA replication.

In summary, we have discovered a small noncoding RNA (ncRNA) that is required to target PRC2 to a specific locus. Long suspected (*18*), an RNA cofactor may explain why no DNA binding subunit for mammalian Polycomb has emerged so far. Ezh2 is apparently the RNA binding PRC2 subunit. For XCI, the data provide new insight into how silencing is initiated on Xi (Fig. 5E). Given Tsix's established role as Xist antagonist (*3*), ability to bind PRC2 and to compete with RepA (Fig. 3), and molar excess over Xist, we propose that Tsix prevents RepA-PRC2 action in pre-XCI cells by titrating RepA away from PRC2, by blocking RepA-PRC2 transfer to chromatin, or by preventing PRC2 catalysis. The last two possibilities may explain why RepA-PRC2 interactions in males do not induce H3-K27me3 (Fig. 1D). In our model, when Tsix is down-regulated on the future Xi, RepA productively engages PRC2, methylates the *Xist* promoter in cis, and enables *Xist* transactivation. In support of this, abolishing Tsix ($Tsix^{\Delta CpG/+}$) results in premature H3-K27 trimethylation (Fig. 1C) and elevated Xist levels (*11*). Full-length Xist also binds PRC2 (Fig. 1), so the spread of Xist RNA along Xi could distribute PRC2 and H3-K27me3 throughout the chromosome. As ectopic *Xist* transgenes are known to spread autosomal silencing (*13*), our data imply that *Xist*—perhaps *RepA* itself (Fig. 1)—serves as a nucleation center. After XCI, Xi maintains its association with PRC2 by means of the perinucleolar compartment in a RepA- and Xist-dependent manner. With evidence that RNA interference is required to localize Xist and target H3-K27me3 (*19*), involvement of small RNAs and RNA interference proteins may also be considered. Because another ncRNA ("HOTAIR") was recently identified in connection with PRC2 at a human HOX locus (*20*), RNA cofactors may emerge as universal requirements for Polycomb targeting.

References and Notes

1. C. J. Brown *et al.*, *Cell* **71**, 527 (1992).
2. G. D. Penny, G. F. Kay, S. A. Sheardown, S. Rastan, N. Brockdorff, *Nature* **379**, 131 (1996).
3. J. T. Lee, N. Lu, *Cell* **99**, 47 (1999).
4. C. M. Clemson, J. A. McNeil, H. Willard, J. B. Lawrence, *J. Cell Biol.* **132**, 259 (1996).
5. J. C. Lucchesi, W. G. Kelly, B. Panning, *Annu. Rev. Genet.* **39**, 615 (2005).
6. L. F. Zhang, K. D. Huynh, J. T. Lee, *Cell* **129**, 693 (2007).
7. K. Plath *et al.*, *Science* **300**, 131 (2003).
8. J. Silva *et al.*, *Dev. Cell* **4**, 481 (2003).
9. A. Kohlmaier *et al.*, *PLoS Biol.* **2**, E171 (2004).
10. L. Ringrose, R. Paro, *Annu. Rev. Genet.* **38**, 413 (2004).
11. B. K. Sun, A. M. Deaton, J. T. Lee, *Mol. Cell* **21**, 617 (2006).
12. B. D. Hendrich, C. J. Brown, H. F. Willard, *Hum. Mol. Genet.* **2**, 663 (1993).
13. A. Wutz, T. P. Rasmussen, R. Jaenisch, *Nat. Genet.* **30**, 167 (2002).
14. T. Sado, Z. Wang, H. Sasaki, E. Li, *Development* **128**, 1275 (2001).
15. N. J. Francis, A. J. Saurin, Z. Shao, R. E. Kingston, *Mol. Cell* **8**, 545 (2001).
16. S. Kalantry, T. Magnuson, *PLoS Genet.* **2**, e66 (2006).
17. S. Schoeftner *et al.*, *EMBO J.* **25**, 3110 (2006).
18. S. Schmitt, R. Paro, *Genome Biol.* **7**, 218 (2006).
19. Y. Ogawa, B. K. Sun, J. T. Lee, *Science* **320**, 1336 (2008).
20. J. L. Rinn *et al.*, *Cell* **129**, 1311 (2007).

21. We thank R. Spencer and Y. Jeon for unpublished data and technical advice and Y. Ogawa for critical reading of the manuscript. Grant support: Massachusetts General Hospital Fund for Medical Discovery (J.Z.), NSF predoctoral award (J.A.E.), Jane Coffin Childs Fellowship (J.J.S.), and NIH-R01GM58839 (J.T.L.). J.T.L. is an Investigator of the HHMI. The transcript "RepA" for Repeat A has GenBank accession number FJ361197.

Supporting Online Material

www.sciencemag.org/cgi/content/full/322/5902/750/DC1
Materials and Methods
Figs. S1 and S2
References

10 July 2008; accepted 19 September 2008
10.1126/science.1163045

Deletion of *Trpm7* Disrupts Embryonic Development and Thymopoiesis Without Altering Mg^{2+} Homeostasis

Jie Jin,[1,2]* Bimal N. Desai,[1]* Betsy Navarro,[1] Adriana Donovan,[2] Nancy C. Andrews,[2,3] David E. Clapham[1]†

The gene *transient receptor potential-melastatin-like 7* (*Trpm7*) encodes a protein that functions as an ion channel and a kinase. TRPM7 has been proposed to be required for cellular Mg^{2+} homeostasis in vertebrates. Deletion of mouse *Trpm7* revealed that it is essential for embryonic development. Tissue-specific deletion of *Trpm7* in the T cell lineage disrupted thymopoiesis, which led to a developmental block of thymocytes at the double-negative stage and a progressive depletion of thymic medullary cells. However, deletion of *Trpm7* in T cells did not affect acute uptake of Mg^{2+} or the maintenance of total cellular Mg^{2+}. *Trpm7*-deficient thymocytes exhibited dysregulated synthesis of many growth factors that are necessary for the differentiation and maintenance of thymic epithelial cells. The thymic medullary cells lost signal transducer and activator of transcription 3 activity, which accounts for their depletion when Trpm7 is disrupted in thymocytes.

The transient receptor potential (TRP) superfamily comprises cation-permeant ion channels that have diverse functions (*1*–*3*). TRPM7 (*1*, *2*) and TRPM6 (*4*, *5*) proteins also contain a C-terminal kinase domain (*6*). TRPM7 is expressed in all examined cell types (*3*) and mediates the outwardly rectifying Mg^{2+}-inhibitable current (MIC) (*7*). TRPM6 and TRPM7 exhibit nearly identical current-voltage (*I-V*) relations, conducting only a few pA of inward current at physiological pH levels (*1*, *2*, *8*, *9*).

A chicken DT-40 B cell line targeted for *Trpm7* gene disruption was reported to require high concentrations of extracellular Mg^{2+} (10 mM) for survival (*10*). Given the permeability of TRPM7 to Mg^{2+}, the results have been interpreted to indicate that TRPM7 was critical for cellular Mg^{2+} homeostasis in vertebrates. A role for TRPM7 in vertebrate development was suggested by a *Danio rerio Trpm7* mutant that exhibited abnormal skeletogenesis and melanophore development, but whether this developmental defect is related to Mg^{2+} homeostasis remains unclear (*11*).

We generated multiple mouse lines with a targeted deletion of the *Trpm7* gene (fig. S1A) (*12*). Mouse lines with disruption of *Trpm7* in all tissues (global deletion), generated using three different approaches, did not yield any live $Trpm7^{null/null}$ animals. Mendelian ratios of littermate genotypes indicated that $Trpm7^{null/null}$

[1]Department of Cardiology, Howard Hughes Medical Institute, Children's Hospital Boston, and Department of Neurobiology, Harvard Medical School, Enders Building 1309, 320 Longwood Avenue, Boston, MA 02115, USA. [2]Division of Hematology and Oncology, Children's Hospital Boston, Karp Family Building 8-125A, Boston, MA 02115, USA. [3]Department of Pediatrics and Department of Pharmacology and Cancer Biology, Duke University School of Medicine, Durham, NC 27702, USA.

*These authors contributed equally to this work.
†To whom correspondence should be addressed. E-mail: dclapham@enders.tch.harvard.edu